Accurate Simulation of Flows with Convected Vortices: Cartesian TAU

Philip Kelleners

DLR, Institute of Aerodynamics and Flow Technology
Lilienthalplatz 7, 38108 Braunschweig, Germany
Philip.Kelleners@dlr.de

Abstract. A fourth order accurate Cartesian solver is being developed for the accurate simulation of flows with convected vortical structures. This Cartesian solver is then used within a zonal approach for simulation of flows in aerospace problems.

Keywords: Higher order scheme, Padé Scheme, Cartesian Solver, Zonal Approach, Chimera, Domain coupling.

1 Accurate Simulation of Convection of Vortical Structures in a Compressible Fluid

Many present day well established aerospace numerical codes, of which the DLR TAU-code is an example, for the simulation of subsonic, transonic or supersonic flow are second order accurate in physical space. For these second order codes it has been observed that freely convecting vortices, amongst other free convected coherent structures, suffer from rapid decay on grids of practical mesh density. The computational cost of accurate simulation of free convected vortices becomes rapidly excessive as the distances over which the vortices travel increase, for these second order accurate codes. Presently designated higher-order methods, that is of spatial order higher than two, are better able to represent these free vortices on grids of moderate density, and thus potentially, could lower the computational cost. However these higher-order methods, in their present state of development, are not well suited to simulate flows with discontinuities like strong shocks in transonic flow, and representation of complex shapes with accurate boundary conditions of order that matches the inner scheme still presents considerable difficulty. A solution is a zonal approach. Within this zonal approach, based on experience, that is best-practice, the flow domain of interest is simulated with different discretization methods each being applied in those regions where their strengths excel. In the implementation of this zonal approach presented, the boundaries of the different grids overlap, and the developing flow state is coupled in these overlapping regions. This procedure is called the Chimera or overset grid approach, and the overlapping grids are also referred to as Chimera grids (see [2]). This zonal approach is illustrated in fig. 1. The DLR TAU-code, a second order accurate method is used for the regions of the flow close to the

N. Kroll et al. (eds.), *Computational Flight Testing*, Notes on Numerical Fluid Mechanics and Multidisciplinary Design 123,
DOI: 10.1007/978-3-642-38877-4_2,

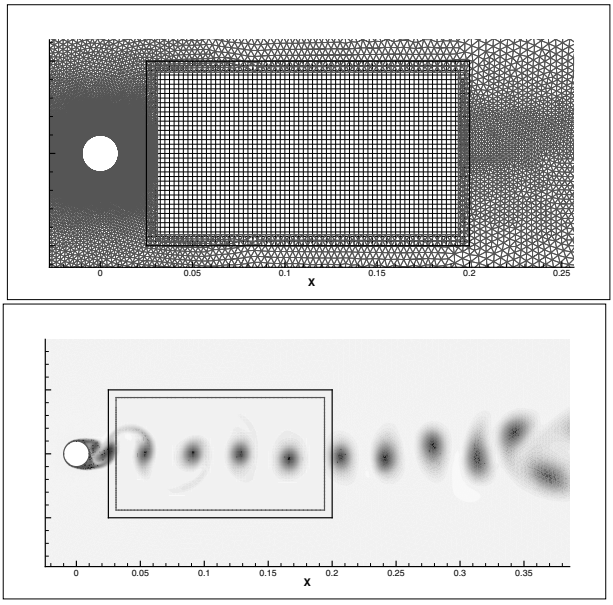

Fig. 1. The von Kármán vortex street behind a circle cylinder. A closeup of the chimera grid in the upper fig., dimensionless entropy-like quantity given by the greyfilled isocontours in the lower fig.

solid geometry. CTAU, the Cartesian grid higher order method presented here, is used on the portion of the grid enclosed by the two boxes. Conservation of the convecting vortices appears to be much better in the domain simulated by the Cartesian solver, as is concluded from the more confined vortex shapes, which start to smear as soon as they leave the Cartesian domain. The difference in quality for the prediction of a convected vortex, between the TAU and the CTAU solutions, will be discussed in more detail in the main text for an isolated vortex in a semi-infinite domain.

As can be seen from the thick black lines, the grids overlap at their boundaries where a code coupling module, (see [7]), performs the exchange of the fluid states and thus implements a strong volume coupling based upon the Chimera technique. The two components of the framework other than the Cartesian Solver are presented briefly below.

1.1 TAU Code

The DLR TAU-code is a fully featured package for simulation of steady and unsteady flow, of both inviscid and viscous compressible fluids, on unstructured hybrid, possibly moving, grids. It implements different turbulence models, overset grid techniques (Chimera), a large number of physical boundary conditions and can efficiently compute solutions on massive parallel computer clusters; e.g. see [6] and `http://tau.dlr.de/`.

1.2 Code2Code Domain Coupling

The Code2Code program (see [7]) is the domain coupling tool, implementing a Chimera boundary between two possibly different CFD-codes, designated code A and code B. The domain coupling is done in three basic steps. There must be a region where the grid domain boundaries of code A and code B overlap. The coefficients for the data-exchange and interpolation for the overlapping region of grids A and B must be computed. At Run-time there must be exchange of the flow-states at the domain boundary grid overlap area at every time level or relaxation step. Code A and code B can be any different code or two instances of the same code.

2 Cartesian Solver, CTAU

The Cartesian solver prototype CTAU is a derivative of the TAU-code. It is a conventional explicit Runge–Kutta based relaxation solver for steady or unsteady flow problems. Discretization of the spatial terms in the equations of fluid flow is done using compact finite difference schemes, or Padé-type schemes, (see [5]), which formally, can be up to tenth order accuracy in space when operating on Cartesian meshes.

2.1 Padé Schemes

As a quick way to illustrate these compact finite difference schemes consider values u_i of a function given at discrete nodes on a regular equidistant one dimensional mesh. Quantities constructed from these nodal values like the derivative u'_i or interpolated values, $u_{1/2}$ inbetween the discrete nodes are computed by *implicit* operators with difference molecules of limited footprint. As an example a first derivative of fourth order accuracy is:

$$u'_{i-1} + 4u'_i + u'_{i+1} = \frac{3(u_{i+1} - u_{i-1})}{h} \quad , \tag{1}$$

where index i designates the position on the regular mesh, u' is the first derivative of u and h is the local meshspacing. The expression for interpolation is:

$$u_{i-1/2} + 6u_{i+1/2} + u_{i+3/2} = 4(u_i + u_{i+1}), \tag{2}$$

which is also fourth order accurate. Inspect the left hand sides of (1) and (2) to check that the derivative or the interpolated values are given in implicit form. For these examples the actual values of the derived or interpolated quantities, at fourth order accuracy, comes at the price of having to solve a tridiagonal system of equations. In the paper of [5] implicit formulations of up to tenth order accuracy of these Padé operators are given of the general form;

$$\beta u'_{i-2} + \alpha u'_{i-1} + u'_i + \alpha u'_{i+1} + \beta u'_{i+2} = a\frac{u_{i+1} - u_{i-1}}{2h} + b\frac{u_{i+2} - u_{i-2}}{4h} + c\frac{u_{i+3} - u_{i-3}}{6h} \quad , \tag{3}$$

where the parameters α, β, a, b and c are derived by matching Taylor series coefficients of various orders. Different schemes of different order of accuracy can be derived for particular combinations of these parameters, again the reader is referred to [5].

2.2 Padé-type Operators for Finite Volume Schemes

The implicit operators introduced above are used in a finite difference context. For the simulation of fluid flow, the conservation properties of the numerical scheme used are of prime importance. Finite-volume schemes are inherently conservative whereas finite difference schemes are not. A finite-volume formulation of the Padé-type scheme, as described by Lacor et all. ([4]), which restores conservation of the dependent, now cell averaged, quantities is implemented in the Cartesian solver presented. The basis for the finite-volume formulation is the definition of *cell-averaged* dependent variables or quantities:

$$\bar{u}_i \equiv \frac{1}{(x_{i+1/2} - x_{i-1/2})} \int_{x_{i-1/2}}^{x_{i+1/2}} u(\xi) d\xi \quad . \tag{4}$$

The fourth order accurate Padé-type operators used as examples before are now expressed in the cell averaged quantity $\bar{u}_i$:

$$u'_{i-1} + 4u'_i + u'_{i+1} = \frac{3(\bar{u}_{i+1} - \bar{u}_{i-1})}{h} \ , \tag{5}$$

for the first derivative, and:

$$u_{i-1/2} + 4u_{i+1/2} + u_{i+3/2} = 3(\bar{u}_i + \bar{u}_{i+1}) \ , \tag{6}$$

for the interpolated values.

Notice how the stencil weights for the interpolated values have changed as a result of application of cell averaged values.

We are concerned with fluid flow. With the finite volume method we need to calculate the fluxes at the interfaces of the control volumes, hence the emphasis on the ability to calculate interpolated values. The fluxes of the Euler and Navier-Stokes equations of motion of fluid are non-linear, as illustrated by a line integral in y-direction for the mass flux in x-direction for two dimensional flow:

$$\int_a^b \rho(x,y) u(x,y) dy \ , \tag{7}$$

which complicates matters considerably as products of the primitive values are not readily available at the volume interfaces. A second order accurate approximation for the flux, averaged over the interface, is:

$$\frac{1}{y_b - y_a} \int_a^b \rho u dy \approx \frac{1}{y_b - y_a} \int_a^b \rho dy \ \frac{1}{y_b - y_a} \int_a^b u dy \ . \tag{8}$$

Additional correction terms of the form $\rho'_x u'_x \frac{\Delta x^2}{12}$ are needed to compute a fourth order accurate flux, where the first derivatives are now evaluated at the interfaces, for the details again refer to [4].

Ghost cells opposite of the domain boundary with quasi cell-averaged values prescribed by the local physical character at the boundary are needed to complete the boundary fluxes.

An implicit assumption for these Padé-type schemes is that argument values and their derivatives exist and are continuous. This is generally not true for discrete initial data, boundary conditions or when flow conditions result in flow structures like e.g. shear regions at length scales which are not resolved by the grid. As a result spurious waves will become part of the discrete solution. These spurious waves are removed effectively from the solution by high-order Padé filters, designed with similar discretization techniques as used for computation of the derivatives, to filter the solution to restore monotone solutions.

To limit the complexity of the current implementation of the Cartesian solver only the Padé-type schemes with parameter β set to zero are considered such that only tridiagonal systems of coupled equations need to be solved. As a consequence the complexity of implementation of the boundary conditions in the ghost cells is reduced.

3 Vortex Model of Ehrenfried

The quality of the results computed with the method described above can be illustrated with the testcase of subsonic convection of a single vortex. Several models for vortices can be found in literature. Vortex models originating from potential flow analysis often have drawbacks as: a non-zero velocity at infinite distance away from the center of the vortex, a singularity at the center of the vortex core with infinite velocity which sometimes is countered by prescribing a solid body rotation at the center of the vortex which in turn may introduce a discontinuity at the interface with the outer, non-corrected, part of the vortex. In [1] Ehrenfried proposed a vortex model for compressible flow which has from none of these drawbacks. The prescribed velocity, density and pressure distributions and all the derivatives of these quantities are continuous which makes the model especially attractive to be used as a test case for a higher order method. As Ehrenfrieds model is not well known, the prescribed distribution for the density and the velocity and pressure relations used in the model are repeated here. The distribution of density is given by:

$$\frac{\rho(r)}{\rho_\infty} = \begin{cases} 1 - \frac{\Delta\rho_v}{2\rho_\infty}\left[1 + \sin\left(\pi\left(1 - \frac{r}{R_0}\right)^3 - \frac{\pi}{2}\right)\right] & \text{for } 0 \le r \le R_0 \\ 1 & \text{for } R_0 < r \end{cases}, \qquad (9)$$

where r is the radial distance from the center of the vortex, R_0 is the bounding radius of the vortex, $\Delta\rho_v$ is the density difference between the center of the vortex core and the undisturbed flow outside of the vortex and the subscript infinity indicates the undisturbed or reference state. Assuming isentropic flow

of an ideal calorically perfect (compressible) fluid throughout all of the domain, the pressure follows from:

$$\frac{p}{p_\infty} = \left(\frac{\rho}{\rho_\infty}\right)^\gamma, \tag{10}$$

and the velocity in circumferential direction, v_θ, follows from the momentum equation in radial direction for rotating steady flow:

$$\frac{dp}{dr} = \frac{\rho v_\theta^2}{r}. \tag{11}$$

4 Testcases

4.1 Inviscid Convection of a Single Ehrenfried Vortex

Consider subsonic parallel flow in x-direction in a 2D domain of dimensions $-16 < x < 16$, $-10 < y < 10$. The domain is of quasi-infinite length in x-direction by application of a periodic boundary condition. At the upper and lower boundaries a farfield state is prescribed. At the initial state $t = 0$ one single Ehrenfried vortex, of radius 8 is superimposed at the origin of the domain. The flow is modeled as inviscid, and for time $t > 0$, the vortex is convected with the initial parallel velocity of Mach = 0.5 in positive x-direction.

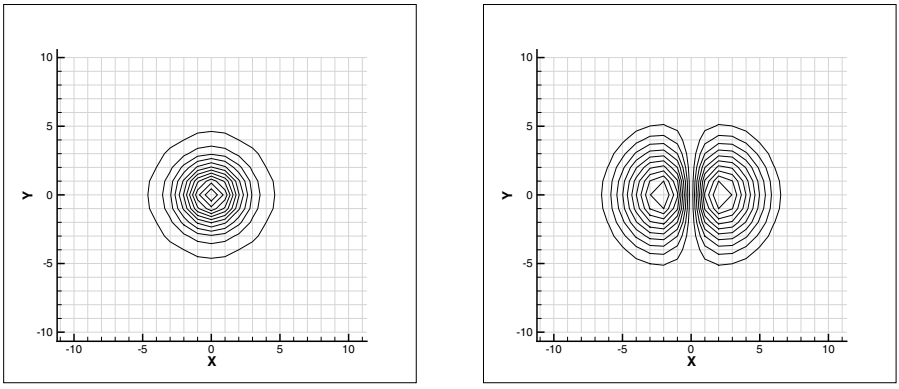

Fig. 2. Initial pressure and y-velocity distributions, for the Ehrenfried vortex model with initial radius 8.0

In simulated time of 0.2 seconds, the vortex moves one time along the complete domain length, crosses the periodic boundaries and arrives at position $x = 1.54$ right of the origin. Two solutions are computed; one with the higher-order method CTAU and one with conventional TAU for comparison, on the same mesh. Additionally, for reference, the initial discretized distribution of the vortex has been moved over the analytic convected distance. What is immediately clear from the left figure 3, is the superior conservation of the vortex

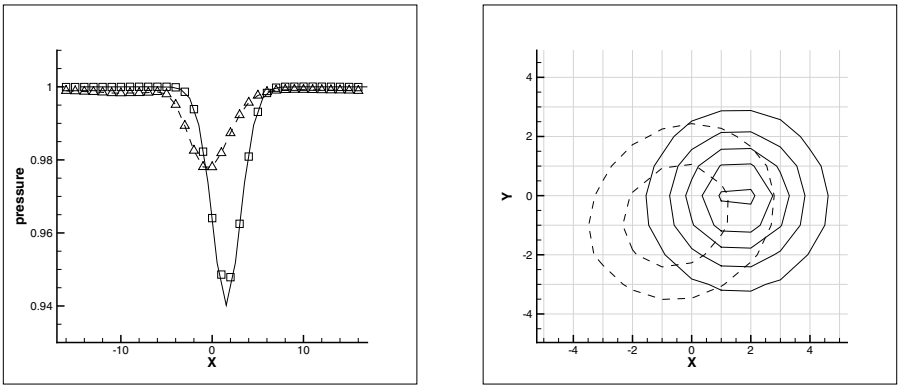

Fig. 3. Convected vortex of Ehrenfried at $t = 0.2$ seconds. Left figure: distribution along the line $y = 0$ for the dimensionless pressure, solid line: transported analytic solution, squares: fourth-order CTAU-solution, dashed line and triangles: second order TAU-solution. Right figure: Iso-contours (pressure) depicting the position of the vortex core, solid lines: CTAU-solution, dashed lines: TAU-solution.

distribution by the higher-order method. Both dissipation and dispersion error of the convected distribution, are very small compared to the distribution computed by the conventional method TAU. The right part of the figure shows that the solution computed with second-order TAU (the dashed lines) fails to accurately predict convection along the x-direction. And whereas the vortex has been noticeable deformed in the TAU-solution, the predictions of position, shape and amplitude of the vortex are of much better quality in the CTAU-computed solution. Evidence of the higher accuracy and better quality of the higher-order solution is also found in figure 4. The density distribution computed with TAU shows noticeable wiggles at the downstream (left-) side of the vortex, where, on this scale, there appear no wiggles in the CTAU-solution. The centerline distribution of the dimensionless velocity in y-direction further illustrates the superior solution computed by CTAU, with no spurious waves apparent in the y-velocity.

4.2 Von Kármán Vortex Street Behind Circle Cylinder

The well known von Kármán vortex street is simulated at a free-stream Mach number of 0.1 at a Reynolds-number of 1000. Both grid and a snapshot at a point in time where the vortex street is well developed are depicted in Fig. 1, the thick black boxes indicate the boundaries of the overlapping grids. The TAU-grid is hybrid with a prismatic layer wrapped around the circle cylinder for good support of the viscous boundary layer and the flow separation at the downstream side close to the cylinder. The vortices are convected with very small losses over the full length of the Cartesian domain, whereas they are quickly dissipated upon further convection in the triangular TAU-grid.

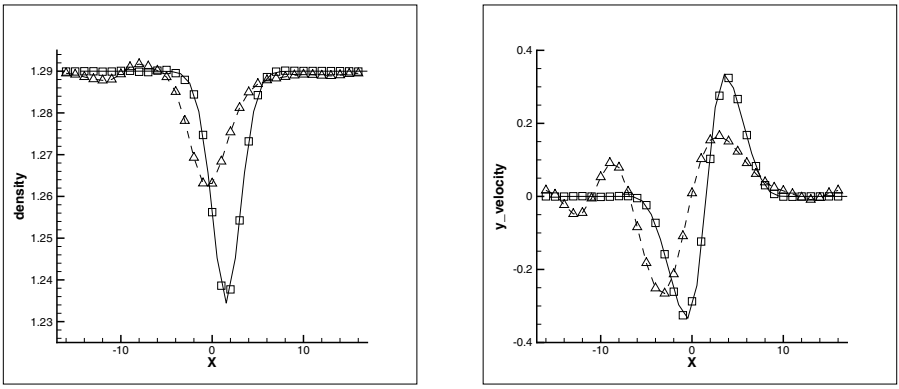

Fig. 4. Convected vortex of Ehrenfried at $t = 0.2$ seconds. Distributions along the line $y = 0$, for density (left) and dimensionless velocity in y-direction (right), solid line: transported analytic solution, squares: fourth order CTAU-solution, dashed line and triangles: second order TAU-solution for comparison.

4.3 Wake Flow Resulting from Transonic Buffet

The configuration of the two airfoils shown in Fig. 5 is a useful approximation to study the effect of the unsteady wake, resulting from transonic wing buffet, as it interacts with a horizontal tailplane. The wing is modeled with the supercritical NLR7301 airfoil of 4.47 meters length at an angle of incidence of three degrees. The horizontal tailplane is modeled with a NACA0012 airfoil of half the wing-chord length at zero degrees angle of incidence. The undisturbed flow is angled at 0.5 degrees, freestream Mach number is 0.73 and the Reynolds number is 26 million. At these conditions shock buffet occurs over the wing airfoil and the unsteady wake influences the pressure distribution at the tailplane consider-

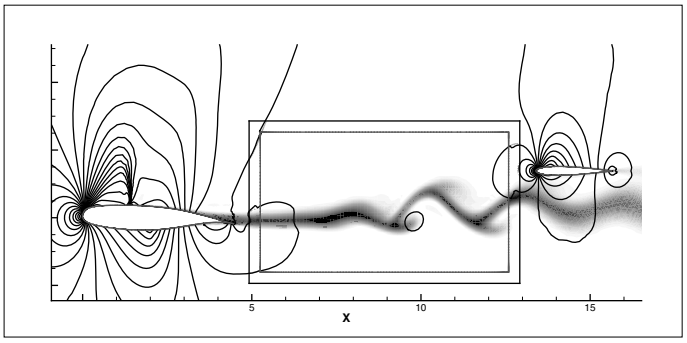

Fig. 5. A snapshot of flow at conditions of transonic buffet; the wake of the wing airfoil interacting with a tailplane airfoil. Greycolored isocontours depict a dimensionless entropy-like quantity, the static pressure is drawn with black isolines, the black boxes show the overlapping boundaries of the chimera grid parts.

ably. Development in the wake of structures of considerable size in the crossflow direction could only be observed in simulations performed with the Cartesian solver inbetween the two airfoils.

5 Conclusions

The fourth order accurate finite volume method CTAU for Cartesian grids has been introduced. The higher order operators for derivative, interpolation and flux reconstruction based on a Padé-type scheme used in the finite volume context have been presented. The superior conservation-, convection properties of the higher order method have been demonstrated successfully for the transport of a single isolated vortex on a semi-infinite domain when compared to a conventional second order method.

A zonal approach for simulation of compressible fluid flow has been presented. Two testcases showing the effective use of the higher order Cartesian method with help of chimera-based domain coupling between two different flow solvers, illustrate the prosperous perspective of the present framework under development. Further work will include testing of the method on full three dimensional configurations and, amongst others, implementation of whirl fluxes to allow for moving meshes, as needed for simulation of rotorcraft.

References

1. Ehrenfried, K., Meier, G.E.A.: Ein Finite-Volumen-Verfahren zur Berechnung von instationären, transsonischen Strömungen mit Wirbeln. Institut für Strömungsmechanik Göttingen, Deutsche Forschungsanstalt für Luft- und Raumfahrt e.V. Forschungsbericht 94-33, ISBN 0939-2963
2. Chesshire, G., Henshaw, W.D.: Composite Overlapping Meshes for the Solution of Partial Differential Equations. Journal of Comp. Physics 90, 1–64 (1990)
3. Kelleners, P.H.: An Edge-based Finite Volume Method for Inviscid Compressible Flow with Condensation. PhD. Thesis University of Twente (December 2007)
4. Lacor, C., Smirnov, S., Baelmans, M.: A finite volume formulation of compact central schemes on arbitrary structured grids. Journal of Comp. Physics 198, 535–566 (2004)
5. Lele, S.K.: Compact Finite Difference Schemes with Spectral-like Resolution. Journal of Comp. Physics 103, 16–42 (1992)
6. Schwamborn, D., Gerhold, T., Heinrich, R.: The DLR TAU-Code: Recent Applications in Research and Industry. Invited Lecture in Proceedings on CD of the European Conference on Computational Fluid Dynamics ECCOMAS CDF (2006)
7. Spiering, F.: Coupling of TAU and TRACE for parallel accurate flow simulations. In: International Symposium “Simulation of Wing and Nacelle Stall", Braunschweig Germany (June 2012)